REPORT No. 709

AN ANALYSIS OF THE STABILITY OF AN AIRPLANE WITH FREE CONTROLS

By Robert T. Jones and Doris Cohen

SUMMARY

An investigation is made of the conditions essential to the stability of an airplane with free control surfaces. Calculations are based on typical airplane characteristics with certain factors varied to cover a range of current designs. Stability charts are included to show the limiting values of the aerodynamic hinge moments and the weight hinge moments of the control surfaces for various positions of the center of gravity of the airplane and for control systems with various moments of inertia. The effects of reducing the chord and of eliminating the floating tendency of the surface, of changing the wing loading, and of decreasing the radius of gyration of the airplane are also indicated. An investigation has also been made of the nature of the motion of the airplane with controls free and of the modes of instability that may occur.

Stability with the controls free generally depends more critically on the design of the control system than on the stability characteristics of the airplane. In particular, too great a weight moment, combined with a high degree of aerodynamic balance, may cause undamped oscillations. Regardless of the weight moment, it appears difficult to secure stability when the aerodynamic balance exceeds 75 percent of the hinge moment.

INTRODUCTION

During recent investigations by the NACA of the flying qualities of several airplanes of different types, a tendency toward longitudinal instability was noted that involved pitching of the airplane reinforced by movements of the elevator. In other flight tests, lateral instability accompanied by oscillations of the rudder or of the ailerons has been noticed. The oscillations observed were rapid enough to be influenced by the inertia of the control surfaces but were not believed to be sufficiently rapid to involve the elasticity of the structure. The problem is thus concerned with motions intermediate between flutter and movements of the airplane as a rigid body.

It was thought that a theoretical analysis of the stability of an airplane with the controls free might shed some light on the cause of these undesirable motions and might indicate how they could be avoided in design. Of the previous publications on the subject, the most detailed is that of E. Bartsch on lateral motions of an airplane with free rudder and ailerons (reference 1). In order to make specific recommendations applicable to modern design, a study of stability more complete and detailed than any available was undertaken. Calculations were made covering both longitudinal and lateral motions and the elevator-free, the rudder-free, and the aileron-free conditions. The computations were based on a set of typical airplane characteristics, except for parameters introduced to cover such variations in control-surface design as seem most likely to affect stability. The results that might be expected under corresponding conditions in airplanes with different over-all mass characteristics have also been indicated.

SYMBOLS AND COEFFICIENTS

The following symbols are used in addition to those defined in the report covers. (See figs. 1 and 2.)

The subscript c refers to a control-surface characteristic and is replaced in the various sections of the report by e for elevator, r for rudder, and a for ailerons; the subscript s refers to the control stick or wheel mechanism.

A length equal to one-half the mean wing chord is used as the fundamental unit of length in order to obtain the results in a form applicable to geometrically similar airplanes of any size or loading. Conversion to this system is made by dividing all lengths measured in ordinary units by the length of the half-wing chord. Quantities entering into nondimensional expressions do not, of course, require such conversion.

U_0 steady-flight speed

β angle of sideslip

k_c radius of gyration of control mechanism about control-surface hinge axis

$\bar{x}_c$ moment arm of center of gravity of control system about hinge axis, positive when center of gravity is behind hinge

$\bar{y}$ distance from center of gravity of aileron to plane of symmetry

A aspect ratio

l tail length of airplane

$x_{a.c.}$ projection on X axis of distance between center of gravity of airplane and its aerodynamic center (with controls fixed)

$\mu = \dfrac{m}{S\frac{\rho}{2}c}$ airplane density ratio

$\mu_c = \dfrac{m_c}{S_c\frac{\rho}{2}c_c}$ control-surface density ratio

ξ aileron weight-moment parameter. (See equation (14).)

H control-surface hinge moment

η control gearing ratio

$C_h = \dfrac{H}{S_c\frac{\rho}{2}U_0^2c_c}$

$s = U_0t$ distance along flight path

$\dot{w}$, $\dot{\delta}$, etc. $= \dfrac{dw}{dt}, \dfrac{d\delta}{dt}$, etc.

$\ddot{\theta}$, $\ddot{\delta}$, etc. $= \dfrac{d^2\theta}{dt^2}, \dfrac{d^2\delta}{dt^2}$, etc.

$D = \dfrac{d}{ds}$ differential operator

$C_{L_\alpha} = \dfrac{\partial C_L}{\partial \alpha}$; $C_{n_\beta} = \dfrac{\partial C_n}{\partial \beta}$; $C_{n_{D\delta}} = \dfrac{\partial C_n}{\partial D\delta}$; etc.

STABILITY WITH ELEVATOR FREE

Pitching motions sufficiently rapid to be affected by the inertia of the elevator control probably will not involve sensible changes in the forward speed of the airplane. Accelerations of the airplane along the flight path will therefore be neglected. The rapidity of the oscillations makes it advisable, on the other hand, to include certain aerodynamic effects not retained in the equations of motion in their usual form. In addition to the moments developed in response to the displacements of the tail surfaces, moments due to angular velocities of these surfaces are also considered. Thus, the pitching moment due to angular velocity of the elevator about its hinge $\partial M/\partial\dot{\delta}$, the pitching moment due to the aerodynamic inertia of the surfaces $\partial M/\partial\dot{w}$, and the aerodynamic damping of the elevator $\partial H/\partial\dot{\delta}$ will be included in the present analysis. Secondary factors entering into the equations, such as the vertical acceleration at the center of gravity due to the lift of the horizontal tail, are neglected. The equations of motion take the following form:

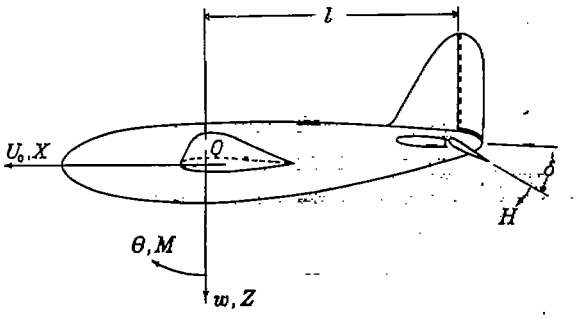

FIGURE 1.—Notation for longitudinal motions.

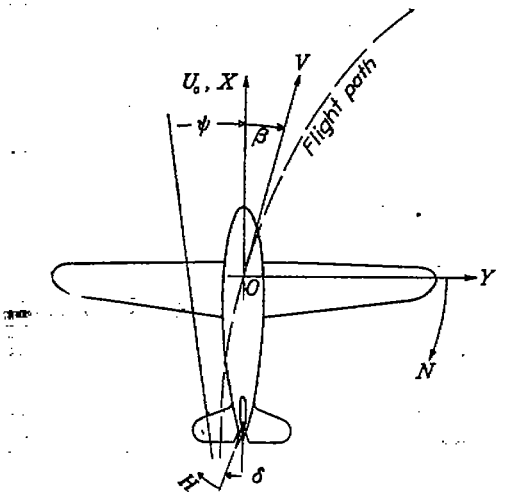

FIGURE 2.—Notation for lateral motions.

$$\left.\begin{aligned}
&m(\dot{w}-U_0\dot{\theta})-w\frac{\partial Z}{\partial w} && =0\\
&mk_Y^2\ddot{\theta}-\dot{\theta}\frac{\partial M}{\partial\dot{\theta}}-w\frac{\partial M}{\partial w}-\dot{w}\frac{\partial M}{\partial\dot{w}}-\delta\frac{\partial M}{\partial\delta}-\dot{\delta}\frac{\partial M}{\partial\dot{\delta}} && =0\\
&m_ek_e^2(\ddot{\delta}+\ddot{\theta})+m_e\bar{x}_e(l\ddot{\theta}+\dot{w}-U_0\dot{\theta})-w\frac{\partial H}{\partial w}-\dot{\theta}\frac{\partial H}{\partial\dot{\theta}} && \\
&\qquad -\delta\frac{\partial H}{\partial\delta}-\dot{\delta}\frac{\partial H}{\partial\dot{\delta}} && =0
\end{aligned}\right\} \quad (1)$$

If the following substitutions are made

$$\mu = \frac{m}{S\frac{\rho}{2}c}$$

$$\mu_e = \frac{m_e}{S_e\frac{\rho}{2}c_e}$$

$$t = \frac{s}{U_0}$$

$$D = \frac{d}{ds} = \frac{1}{U_0}\frac{d}{dt}$$

$$w = \alpha U_0$$

$$\frac{c}{2} = 1$$

and the stability derivatives are replaced by the equivalent coefficients, equations (1) are reduced to the following nondimensional form:

$$\left.\begin{aligned}
&\left(\mu D+\frac{C_{L_\alpha}}{2}\right)\alpha-\mu D\theta &&=0\\
&-(C_{m_{D\alpha}}D+C_{m_\alpha})\alpha+(\mu k_Y{}^2D-C_{m_{D\theta}})D\theta\\
&\qquad-(C_{m_{D\delta}}D+C_{m_\delta})\delta &&=0\\
&(\mu_e\bar{x}_eD-C_{h_\alpha})\alpha+[\mu_e(\bar{x}_el+k_e{}^2)D-\mu_e\bar{x}_e-C_{h_{D\theta}}]D\theta\\
&\qquad+(\mu_ek_e{}^2D^2-C_{h_{D\delta}}D-C_{h_\delta})\delta &&=0
\end{aligned}\right\} \quad (2)$$

It is to be noted that, with the exception of the independent variable s, equations (2) involve no quantities dependent on the steady-flight speed. Motions plotted against the distance s are therefore applicable to any initial flight condition within the unstalled range.

The equations of motion are based on the assumption of a constant forward velocity and therefore do not show the possibility of a phugoid oscillation of increasing amplitude or the possibility of a certain type of slow divergence from the steady-flight attitude. Experience has shown that the unstable phugoid motion is not likely to cause trouble under ordinary operating conditions because its period is of the order of 2500 chord lengths; the oscillations of interest in control-free stability have periods of the order of 50 chord lengths. The slow divergence corresponds simply to a loss of static stability when the control is free. Static stability with the elevator free is assured if the following condition is fulfilled:

$$C_{h_\delta}C_{m_\alpha}>C_{m_\delta}C_{h_\alpha} \quad (3)$$

In this paper the divergence treated is of a more rapid type.

Because the pitching that enters into the equations of motion was expected to be quite rapid, it was thought that the lag in the effect of the wing wake at the tail would be an important factor. Under steady conditions, the wing wake diminishes the relative angle of attack at the tail to about one-half. After a sudden change of angle, however, the tail will at first receive a strong upwash due to vortices shed by the wing in consequence of its additional circulation. The result is a rather complex transient variation of the vertical velocity. This variation affects both the lift of the horizontal tail and the floating moment of the elevator.

The possible effect of the transient-flow phenomenon at the tail was estimated by making several calculations in which a simple fixed lag in the action of the downwash was assumed, expressed by setting [1]

$$C_{m_\alpha}=C_{m_{\alpha_{wing}}}+C_{m_{\alpha_{tail}}}(1-\epsilon_\alpha e^{-lD}) \quad (4)$$

$$C_{h_\alpha}=C_{h_{\alpha_{tail}}}(1-\epsilon_\alpha e^{-lD}) \quad (5)$$

A comparison of the resulting motions with corresponding results obtained when the lag function was entirely omitted showed that the lag, although having a noticeable effect on certain stable modes of oscillation, caused only a small change in the slower type of oscillation in which instability occurs first. Revision of the computations to include a more accurate representation of the lag was therefore considered not worth while and all calculations were allowed to stand with $\epsilon_\alpha e^{-lD}$ as the lag operator. In order to combine this operator with other terms of the equations, the expression was expanded into a power series in D.

The stability of the motions is indicated by the nature of the roots of the characteristic equation, which is obtained from equations (2) by setting the determinant formed from the coefficients equal to zero. If $D\theta$, rather than θ, is considered one of the variables, this equation is

$$\begin{vmatrix}
\mu D+\frac{1}{2}C_{L_\alpha} & -\mu & 0\\
-C_{m_{D\alpha}}D-C_{m_\alpha}(D) & \mu k_Y{}^2D-C_{m_{D\theta}} & -C_{m_{D\delta}}D-C_{m_\delta}\\
\mu_e\bar{x}_eD-C_{h_\alpha}(D) & \mu_e(\bar{x}_el+k_e{}^2)D-\mu_e\bar{x}_e-C_{h_{D\theta}} & \mu_ek_e{}^2D^2-C_{h_{D\delta}}D-C_{h_\delta}
\end{vmatrix}=0 \quad (6)$$

The equation is thus a quartic, and terms introduced by the expansion of $C_{m_\alpha}(D)$ and $C_{h_\alpha}(D)$ that would increase its degree were discarded because the roots are always small and higher powers are negligible in value.

The roots of the stability equation were found for several typical cases. Apparently, in the usual case the motion is oscillatory and of two fairly distinct modes. One of the modes of oscillation, although more rapid than the modes encountered with the controls fixed, is nevertheless slow enough (with a period of the order of 60 chord lengths) to involve coupling and reinforcing movements of the airplane. The damping is consequently light, and instability will occur first in this slower mode. It is undoubtedly this mode that has been observed in flight in the cases mentioned in the introduction. The second mode is much more rapid but heavily damped. The short period (about 15 chord lengths) suggests that the motion is essentially limited to a flapping of the elevator and may become unstable only as flutter involving elastic deformations of the structure.

It was expected that variations in the aerodynamic hinge-moment slope C_{h_δ}, the mass-moment coefficient $\mu_e\bar{x}_e$, the moment-of-inertia coefficient $\mu_ek_e{}^2$, and the static stability coefficient C_{m_α} would be most important from the designer's point of view. These quantities were therefore retained in the equations as parameters, and numerical values were substituted for the remaining quantities. Limiting conditions for stability are then in the form of relations connecting the four variables.

Of the conditions for stability, only two were found to be effective within the practical range of the parameters. A boundary beyond which straight divergence

[1] For the use of the operator e^{-lD} to show the effect of lag, see reference 2, page 26. Subsequent investigation (reference 3) has shown the complex transient effect to be more nearly approximated by the operator $\epsilon_\alpha e^{-(l+\frac{1}{2})D}$.

occurs is obtained by setting the constant term of the stability equation

$$\mu(C_{h_\delta}C_{m_\alpha}-C_{m_\delta}C_{h_\alpha})+\frac{C_{L_\alpha}}{2}[C_{h_\delta}C_{m_{D\theta}}-C_{m_\delta}(C_{h_{D\theta}}+\mu_e\bar{x}_e)] \quad (7)$$

equal to zero. This expression is independent of the elevator moment of inertia. The second boundary is the limit for oscillatory stability and is obtained by applying Routh's discriminant to the stability quartic. This boundary was found to shift only a negligible amount with a large change in the static-stability coefficient C_{m_α} and was therefore considered to be independent of C_{m_α}. Partial elimination of the parameters in this way made possible the presentation of the results in a simplified form.

The computations of figure 3 were based on the characteristics of generally used types of balance and on a set

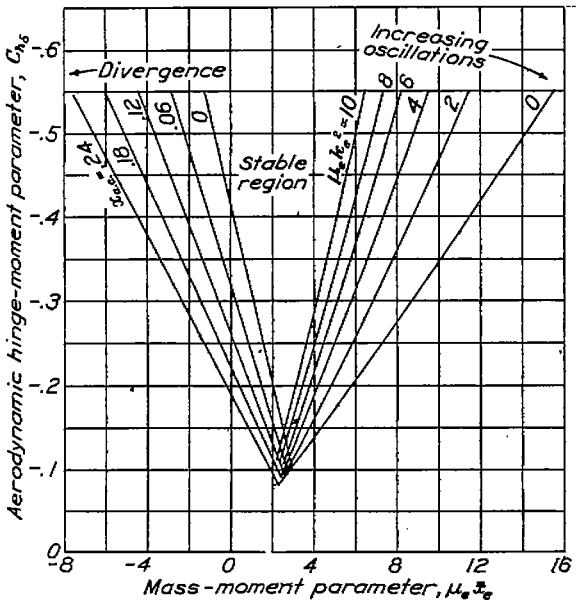

FIGURE 3.—Elevator-free stability regions. 50-percent-chord elevator; μ, 45; k_Y, 1.79.

of typical airplane characteristics. (See table I of the appendix.) The effect of variation of the moment of inertia was subsequently investigated. Figure 4 covers the case of an airplane with the radius of gyration reduced to make the moment of inertia half the average assumed for figure 3. An investigation was also made of the stability of a more heavily loaded airplane by doubling the density factor μ and comparing (fig. 5) a representative stability boundary (in terms of $\mu_e k_e^2$ and $\mu_e\bar{x}_e$) with the corresponding curve for the conditions of figure 3. The particular variations chosen were considered representative of the trends in modern airplane design.

Of the over-all characteristics of an airplane, the radius of gyration seems most likely to affect its stability. The results show that an airplane with a small radius of gyration will not permit so wide a range of the elevator design parameters as will the assumed average airplane. Its greater responsiveness to elevator deflection will cause it to reinforce more readily the movements of the elevator leading to oscillatory instability. The boundary for divergence (equation (7)) is independent of variations in the radius of gyration.

As shown in figure 5, the relative density or loading

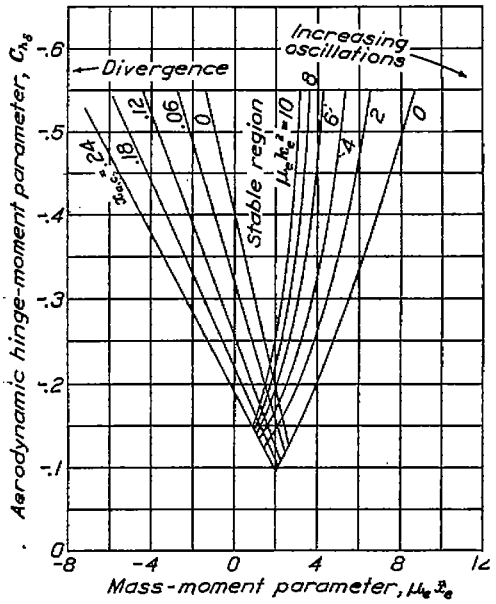

FIGURE 4.—Elevator-free stability. Regions for reduced airplane moment of inertia. 50-percent-chord elevator; μ, 45; k_Y, 1.27.

of the airplane is not a critical factor, which may be attributed to the fact that the normal relation between the lift-curve slope and the loading is such that the airplane is effectively constrained against relative motions normal to the wing surface. Differences in the

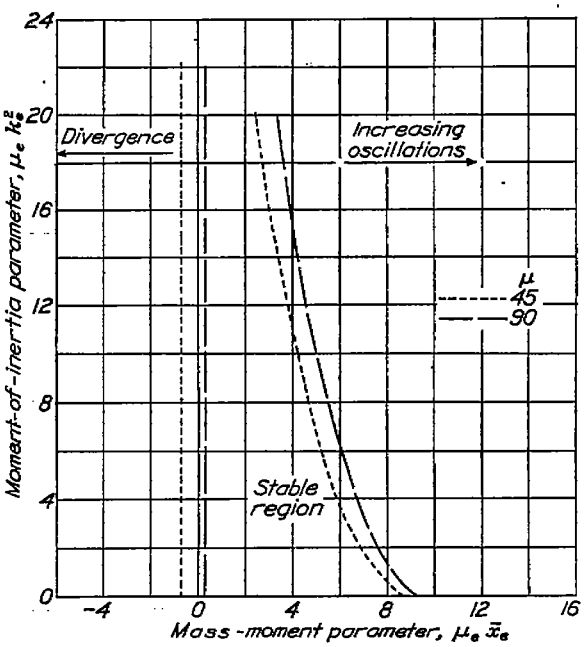

FIGURE 5.—Elevator-free stability. Effect of increasing density factor. C_{h_δ}, ; $x_{a.c.}$, 0.12; k_Y, 1.79.

degree of this constraint, as caused by ordinary variations in either C_{L_α} or μ, are unimportant.

In general, it may be concluded that the design of the elevator itself is of critical importance in obtaining control-free stability. A large mass moment or moment of inertia of the control surface is seen to be unfavorable

to stability. Of primary concern, however, is the adverse effect of aerodynamic balance, especially because it is found necessary to resort to a high degree of balance with many modern airplanes.

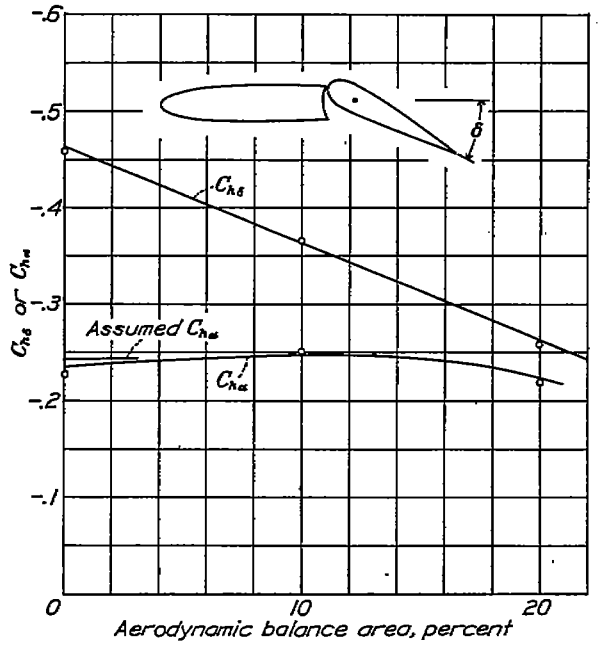

FIGURE 6.—Typical variation of C_{h_δ} and C_{h_α} with aerodynamic balance area for small deflections (from reference 4).

Figure 6 (taken from data of reference 4) shows typical hinge-moment-coefficient curves for a control flap having the inset-hinge type of balance used in most modern control systems. In these experiments, the hinge moment due to a unit change in the angle of attack

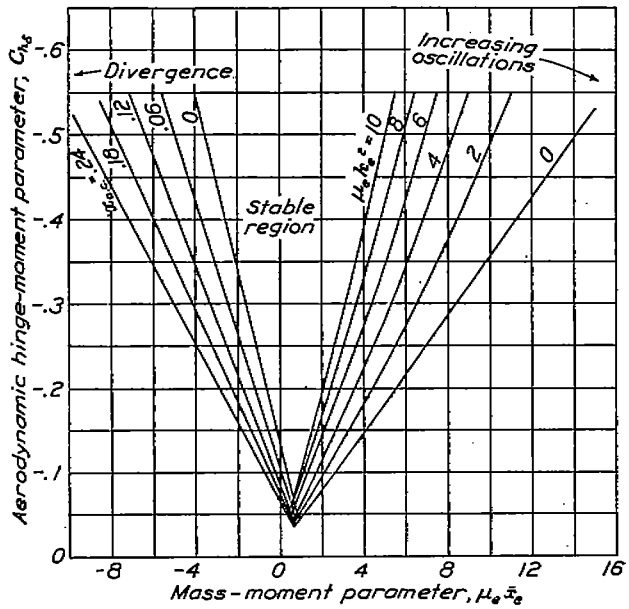

FIGURE 7.—Elevator-free stability. Regions for nonfloating elevator. 50-percent-chord elevator; μ, 45; k_Y, 1.79.

remained practically constant as the balance area was increased. This form of balance thus would not provide compensation for the floating moment C_{h_α} in the same proportion as for the restoring moment C_{h_δ} and, as the degree of balance was increased, the equilibrium floating angles would become increasingly large, so that there would be greater danger of static instability with controls free, as shown in equation (3). The same considerations apply to the balancing tab.

On the other hand, it should be possible to compensate for the floating pressure in the same or, perhaps, in a greater proportion than the proportion of reduction of the restoring moment. Thus, with a horn type of balance, for example, the equilibrium floating angles may be held constant or may even be reduced, which results in greater static stability.[2] A comparison of figure 3 ($C_{h_{\alpha_{tail}}} = -0.24$) with figure 7 ($C_{h_{\alpha_{tail}}} = 0$) shows that decreasing the floating moment also decreases the likelihood of rapid divergence. The boundary for oscillatory stability is hardly influenced by this factor.

The computations for either type of balance apply to an elevator operated by a servo tab, provided that

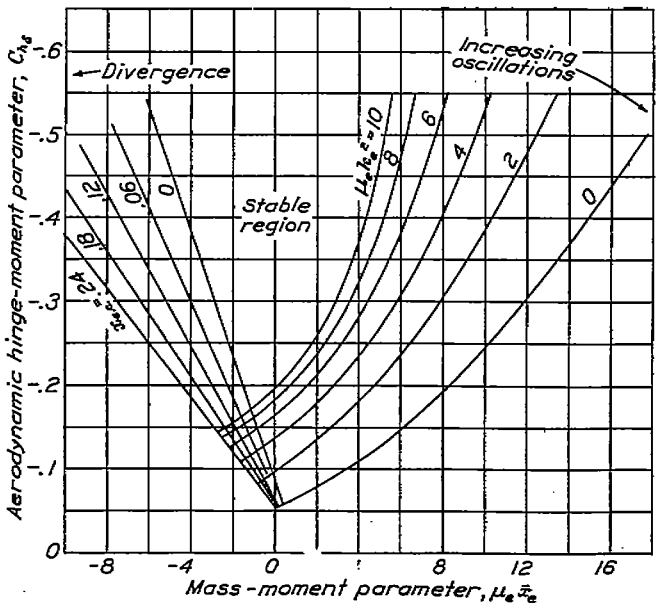

FIGURE 8.—Elevator-free stability. Regions for reduced elevator chord. 25-percent-chord elevator; μ, 45; k_Y, 1.79.

the tab remains fixed relative to the elevator during the oscillations. Thus, as far as stability is concerned, servo operation with controls fixed corresponds to the ordinary control-free condition. The stability with both elevator and servo tab free is not covered in the present study.

Future designs will probably show a trend toward narrower control surfaces, whether balanced or not, because the basic hinge moments can be markedly reduced with a small loss of effectiveness. If the chord of the elevator is reduced from 50 percent to 25 percent of that of the horizontal tail surface, its effectiveness is reduced by only 30 percent; whereas, the basic hinge moment is divided by 4.

Figure 8 shows the regions of stability with a reduced

[2] Another advantage of the horn type of balance is that the hinge gap may be sealed. The subject of horn balances is discussed further by Hemphill in reference 5.

elevator chord. The differences between these regions and those of figure 3 are principally due to changes in the coefficients $\partial C_h/\partial\alpha$, $\partial C_h/\partial D\delta$, and $\partial C_m/\partial D\delta$. As previously noted, the control moment (proportional to $\partial C_m/\partial\delta$) is reduced by only 30 percent. In the interpretation of this figure, it should be borne in mind that the ratios $\bar{x}_e$ and k_e would naturally be smaller for the narrower elevator. If account were taken of this scale factor, the region of stability would appear much wider than the region for the 50-percent elevator.

An effective method of obtaining greater stability in the control-surface motions is the introduction of additional damping into the system. If the responsiveness of the control surface is reduced, a considerably larger degree of aerodynamic balance may be used (fig. 9). The permissible mass unbalance is also increased, although to a lesser extent. The results

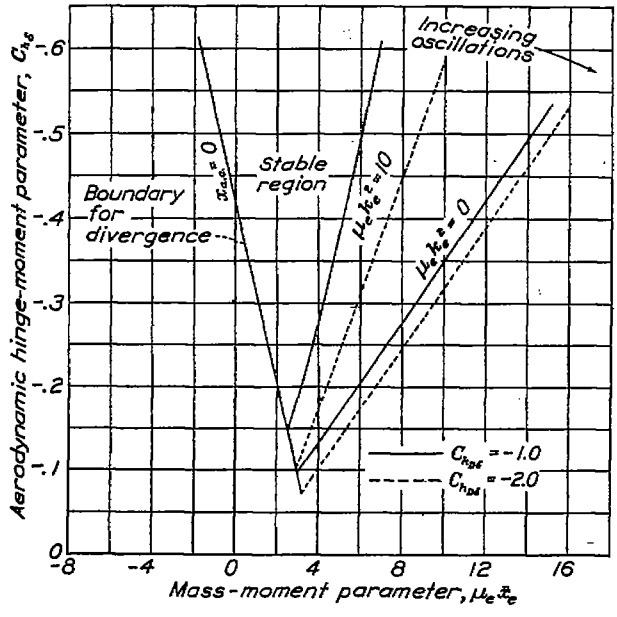

FIGURE 9.—Elevator-free stability regions. Effect of additional damping in the control system. 50-percent-chord elevator; μ, 45; k_r, 1.79.

shown are for a comparatively small amount of damping ($\Delta C_{h_{D\delta}} = -1.0$), which corresponds, for a rate of deflection of 20° per second, to the force required of the pilot to maintain 1° of elevator deflection.

STABILITY WITH RUDDER FREE

Because the lateral motions involve two controls and five degrees of freedom, the analysis is more complex than for the longitudinal motion, which has one control and three degrees of freedom. Fortunately, the rudder and the ailerons exert their principal influences on different modes and only a slight loss in accuracy is incurred if each mode is treated separately.

Oscillation of the rudder control will be primarily influenced by coupling with the yawing oscillations of the airplane. The small rolling oscillations simultaneously induced will generate neither very strong yawing moments nor very strong rudder hinge moments; hence, the rolling degree of freedom will be neglected in the examination of rudder-free stability. This assumption, which has been checked quantitatively by Bartsch (reference 1), reduces the simultaneous equations of motion to the following form:

$$\left.\begin{aligned} &mU_0(\dot{\psi}+\dot{\beta})-\beta\frac{\partial Y}{\partial\beta} &&=0\\ &mk_z^2\ddot{\psi}-\dot{\psi}\frac{\partial N}{\partial\dot{\psi}}-\beta\frac{\partial N}{\partial\beta}-\delta\frac{\partial N}{\partial\delta}-\dot{\delta}\frac{\partial N}{\partial\dot{\delta}} &&=0\\ &m_r k_r^2(\ddot{\psi}+\ddot{\delta})-m_r\bar{x}_r U_0(\dot{\psi}+\dot{\beta})+lm_r\bar{x}_r\ddot{\psi}-\beta\frac{\partial H}{\partial\beta}-\delta\frac{\partial H}{\partial\delta}\\ &\qquad -\dot{\delta}\frac{\partial H}{\partial\dot{\delta}}-\dot{\psi}\frac{\partial H}{\partial\dot{\psi}} &&=0 \end{aligned}\right\} \quad (8)$$

If substitutions corresponding to those introduced in the elevator calculations are made, the equations are reduced to the following nondimensional form:

$$\left.\begin{aligned} &\left(\mu D-\frac{C_{Y_\beta}}{2}\right)\beta+\mu D\psi &&=0\\ &-C_{n_\beta}\beta+\left(\frac{\mu k_z^2 D}{A}-C_{n_{D\psi}}\right)D\psi-(C_{n_{D\delta}}D+C_{n_\delta})\delta &&=0\\ &-(\mu_r\bar{x}_r D+C_{h_\beta})\beta+[\mu_r(k_r^2+\bar{x}_r l)D-(C_{h_{D\psi}}+\mu_r\bar{x}_r)]D\psi\\ &\qquad +(\mu_r k_r^2 D^2-C_{h_{D\delta}}D-C_{h_\delta})\delta &&=0 \end{aligned}\right\} \quad (9)$$

The stability equation is

$$\begin{vmatrix} -\mu D+\frac{C_{Y_\beta}}{2} & \mu & 0\\ C_{n_\beta} & \frac{\mu k_z^2 D}{A}-C_{n_{D\psi}} & -(C_{n_{D\delta}}D+C_{n_\delta})\\ \mu_r\bar{x}_r D+C_{h_\beta} & \mu_r(k_r^2+\bar{x}_r l)D & \mu_r k_r^2 D^2\\ & -(C_{h_{D\psi}}+\mu_r\bar{x}_r) & -C_{h_{D\delta}}D-C_{h_\delta} \end{vmatrix}=0 \quad (1$$

This equation is closely analogous to equation (6) for longitudinal motion. The corresponding coefficients have similar values with the exception of C_{Y_β}, which is much smaller than the corresponding term C_{L_α} because the normal force that is developed by the wing in pitching is absent in the lateral motions.

The roots of the stability equation again indicate two modes of motion. Thus, in a typical case, the roots are $-0.008\pm0.035i$ and $-0.25\pm0.28i$. In this instance, the modes are both oscillatory. The first pair of roots indicates a lightly damped oscillation of such a frequency (period≅90 chord lengths) as to involve sensible coupling between the yawing of the airplane and the swinging of the rudder. The second mode is of much higher frequency and undoubtedly represents the natural oscillation of the rudder with the airplane acting as a practically rigid support. When the restoring moment C_{h_δ} is reduced, the second mode becomes aperiodic and eventually divergent as the motion becomes less rapid. Oscillatory instability appears first in the slower mode, as in the case of the elevator.

Page 115, Figures 10 to 13: All values of C_{n_β} given in figures 10 through 13 should be reduced by dividing by 6; that is, the values on the curves should read C_{n_β} = 102, .064, and .026 instead of .612, .384, and .156.

Page 116: In the second equation of the two bracketed as (12), the sign of the third term should be changed from minus to plus; thus the equation should read:

$$m_a k_a^2 \frac{d^2\delta}{dt^2} - p\frac{\partial H}{\partial p} + \frac{dp}{dt}(m_a\overline{yx} + \ldots$$

Pages 116 and 117: Figure 14, containing the aileron-free stability boundaries, has been found to be incorrect and should not be used. The paragraph referring to this figure, beginning at the bottom of page 116 and continuing through equation (15) on page 117, is therefore also in error. The correct boundaries for oscillatory stability with ailerons free are given in a new figure 14 which has been inserted in this copy of the Annual Report. The boundary for divergence is that given by equation (16). Statement 3 under "Concluding Remarks," page 117, no longer applies to ailerons.

The calculations of the stability boundaries covered changes in rudder chord, changes in the airplane moment of inertia mk_Z^2, and changes in the weathercock stability factor C_{n_β}. Additional calculations were made to show the action of a nonfloating type of rudder.

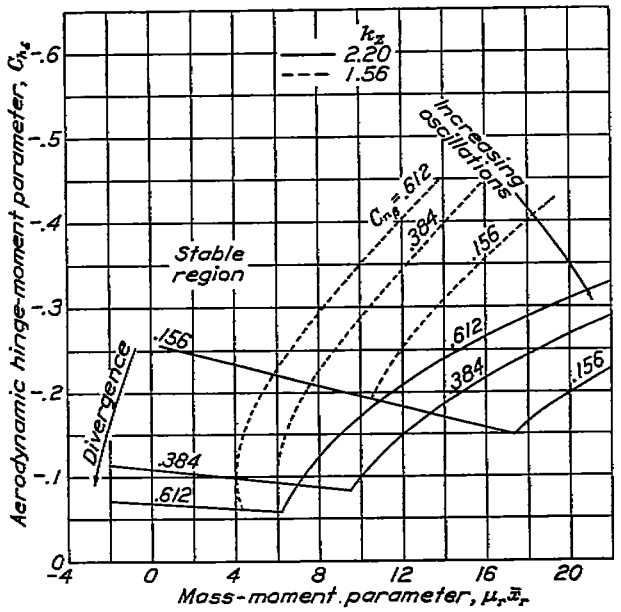

FIGURE 10.—Rudder-free stability. Minimum regions ($0<\mu_r k_r^2<8$). 50-percent-chord rudder; μ, 45.

Variations in the density factor μ were considered insignificant, this quantity entering the equations independently only in conjunction with the small side-force derivative C_{Y_β}.

A simplification corresponding to the elimination of

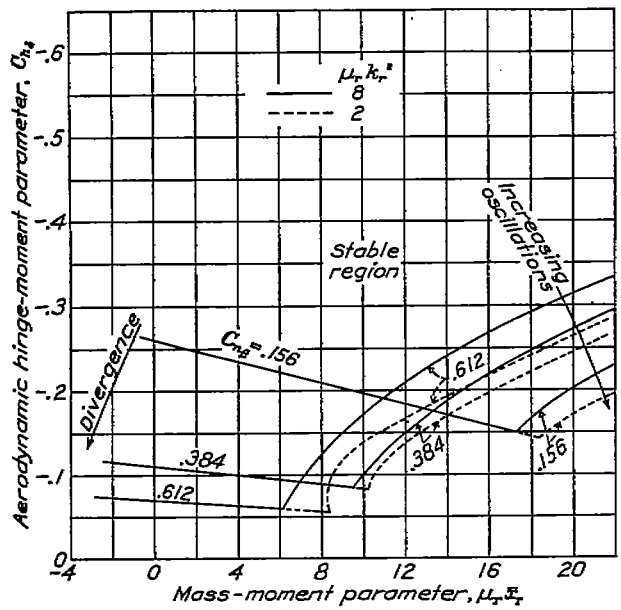

FIGURE 11.—Rudder-free stability. Variation of boundaries with moment of inertia of rudder. 50-percent-chord rudder; μ, 45; k_Z, 2.20.

C_{m_α} as a parameter of the oscillatory stability boundary was not found possible in these equations. Plots of Routh's discriminant for rudder-free motion show it to be noticeably dependent on all four parameters, the least effective being the moment of inertia of the rudder system. Since the permissible mass moment is smaller for larger values of $\mu_r k_r^2$, an upper practical limit ($\mu_r k_r^2<8$) was assumed for this parameter and the resulting family of curves was plotted to give the minimum regions for stability in terms of C_{h_δ}, $\mu_r\bar{x}_r$,

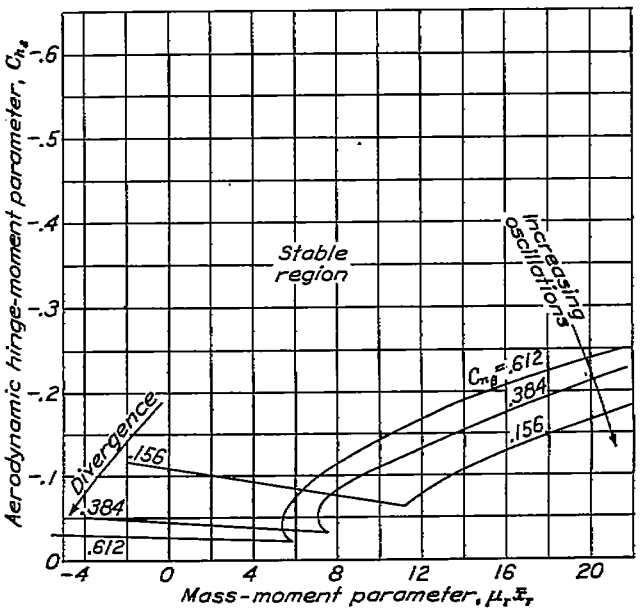

FIGURE 12.—Rudder-free stability. Minimum regions for reduced rudder chord ($0<\mu_r k_r^2<8$). 25-percent-chord rudder; μ, 45; k_Z, 2.20.

and C_{n_β} (figs. 10, 12, and 13). The margin beyond these minimum regions, for values of $\mu_r k_r^2$ less than 8, is indicated by figure 11, in which the corresponding curves for $\mu_r k_r^2=8$ and $\mu_r k_r^2=2$ are plotted.

The charts show the weathercock stability of the air-

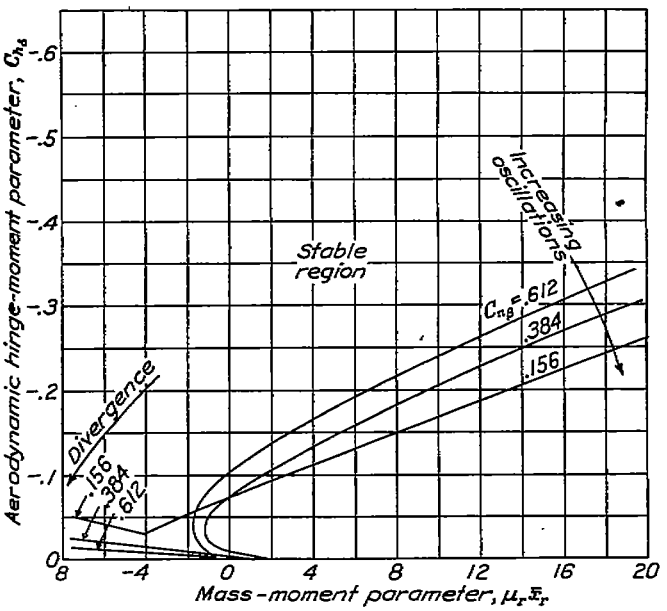

FIGURE 13.—Rudder-free stability. Minimum regions for nonfloating rudder. ($0<\mu_r k_r^2<8$). 50-percent-chord rudder; μ, 45; k_Z, 2.20.

plane to be of greater importance in the case of lateral motion than in the case of longitudinal motion. The effect of the moment of inertia of the control surface, which determined the degree of oscillatory stability in longitudinal motion, is small relative to the effect of

C_{n_β}. The greater the value of C_{n_β}, the less is the allowable mass moment with any given amount of aerodynamic balance. On the other hand, if the mass moment is small enough to insure damping of the oscillations, a larger value of C_{n_β} will increase the aerodynamic balance that may be introduced without causing divergence. The radius of gyration of the airplane is of considerable importance, shifting the boundary for oscillatory stability so as very nearly to double the stable region when the moment of inertia is doubled. (See fig. 10.)

Instability with the rudder free is likely to occur in the form of a divergence. The criterion is practically the same as the condition for weathercock stability with the control free, which is

$$C_{h_\delta}C_{n_\beta}-C_{h_\beta}C_{n_\delta}\geqq 0 \tag{11}$$

This criterion is independent of the moments of inertia of the airplane and of the control surface. The greatest

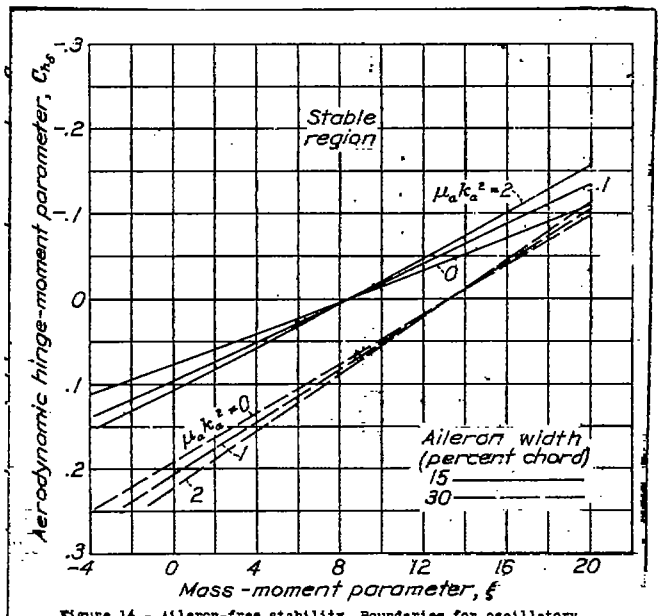

Figure 14.- Aileron-free stability. Boundaries for oscillatory stability. μ, 45; k_x, 1.60.

gain in this margin of stability is obtained by increasing C_{n_β} and reducing the floating tendency C_{h_β} of the rudder. Reducing the chord of the rudder decreases both C_{h_β} and C_{n_δ} and hence considerably widens the margin of stability. (See fig. 12.) Complete elimination of C_{h_β} by the use of a nonfloating type of balance eliminates the likelihood of divergence within the normal range of weight distribution (fig. 13). Such a gain, however, would be achieved only by sacrificing some margin of oscillatory stability.

The lateral oscillations of an airplane with controls fixed are known to be influenced by coupling between the rolling and the yawing motions. These oscillations tend to become undamped when the weathercock stability C_{n_β} approaches zero. Freeing the rudder control diminishes C_{n_β} and may thus lead to this type of oscillatory instability. The condition for zero weathercock stability is approximately that for straight divergence in the control-free condition (equation (11)) and the boundaries for divergence (figs. 10 to 13) can therefore be interpreted also as boundaries for stability of the slow lateral oscillation, when the airplane is free to roll. The absence in the criterion of terms involving the mass of the rudder may be explained by the fact that, as the limit of stability is approached, the oscillation becomes very slow and the yawing component tends to disappear.

STABILITY WITH AILERONS FREE

The stability of an airplane with the ailerons free is examined by including in the equations the interaction between rolling motions of the airplane and movements of the ailerons. Small simultaneous yawing and sideslipping motions will also occur but, because their reactions on the rolling and the hinge moments are small, they may be neglected. The resulting equations are:

$$\left.\begin{aligned} mk_x^2\frac{dp}{dt}-p\frac{\partial L}{\partial p}-\delta\frac{\partial L}{\partial \delta}-\dot{\delta}\frac{\partial L}{\partial \dot{\delta}} &=0\\ m_a k_a^2\frac{d^2\delta}{dt^2}-p\frac{\partial H}{\partial p}-\frac{dp}{dt}(m_a\bar{y}\bar{x}+\eta m_s k_s^2)-\delta\frac{\partial H}{\partial \delta}-\dot{\delta}\frac{\partial H}{\partial \dot{\delta}} &=0 \end{aligned}\right\} \tag{12}$$

or, in nondimensional form,

$$\left.\begin{aligned} \left(\frac{\mu k_x^2}{A}D-C_{l_{D\phi}}\right)D\phi-(C_{l_{D\delta}}D+C_{l_\delta})\delta &=0\\ (\xi D-C_{h_{D\phi}})D\phi+(\mu_a k_a^2 D^2-C_{h_{D\delta}}D-C_{h_\delta})\delta &=0 \end{aligned}\right\} \tag{13}$$

In the aileron control, a part of the mechanism normally rotates about an axis at right angles to the aileron hinge axis. As a result, a part of the aileron torque produced by angular acceleration of the airplane is proportional to the product of inertia of the aileron itself and another part is proportional to the moment of inertia of the control stick or wheel. Both quantities are included in the parameter ξ. Thus:

$$\xi=\frac{m_a\bar{y}\bar{x}+\eta m_s k_s^2}{S_a\frac{\rho}{2}c_a} \tag{14}$$

where the subscript s refers to the control stick and η is a constant inserted to take account of any difference of gearing between the control and the aileron.

The calculations, based on values of the derivatives given in the appendix, cover two aileron widths: 15 percent and 30 percent of the wing chord. In both cases, the ailerons were assumed to cover 50 percent of the wing semispan.

Variations in the floating tendency of the aileron were also considered but were found to have little effect on the stability. The results given may therefore be applied to any of the existing types of balance that give smooth hinge-moment curves.[3]

The boundaries for stability in the two possible modes are presented in figure 14. Instability appears

[3] Certain ailerons of the Frise type that show a reversal of the hinge-moment slope may develop uncontrollable oscillations of fixed amplitude. This condition is discussed in reference 6.

in the form of increasing oscillations and is most likely to occur when the ailerons have a high degree of aerodynamic balance and too great a mass moment or moment of inertia. As the moment of inertia decreases, the boundary for undamped oscillations approaches that for straight divergence (which is itself independent of the moment of inertia); and it becomes possible for both types of instability to exist simultaneously. The condition to prevent straight divergence,

$$C_{l_\delta}\xi - C_{h_{D_\phi}}C_{l_{D\delta}} - C_{l_{D\phi}}C_{h_{D\delta}} - \frac{1}{A}C_{h_\delta}\mu k_x^2 > 0 \qquad (15)$$

is, however, always satisfied when there is damping of the oscillations.

Straight divergence, as encountered in the elevator-free and the rudder-free conditions, is indicated when the constant term of the stability equation is negative, that is, when

$$C_{l_{D\phi}}C_{h_\delta} \gtrless C_{h_{D\phi}}C_{l_\delta} \qquad (16)$$

This condition is not likely to occur unless the aerodynamic balance is nearly complete.

CONCLUDING REMARKS

Experience has shown that, before the actual limit of stability is reached, the airplane undergoes oscillations which, although damped, are still persistent enough to be undesirable. The boundaries given in the stability charts are therefore of value chiefly as indications of the effect of certain design factors; they are useful quantitatively only as outside limits, not to be approached too closely. Further experiments will be necessary to determine the margin of stability required for smooth operation in gusty air.

On the other hand, the charts are to a certain extent conservative because they do not take into account the possibility of friction of the control system, a factor that would widen the margin of stability.

The indications of the present study may be summarized as follows:

1. There is a limit to the effectiveness of the aerodynamic balance that may be safely employed with any conventional control system. In most cases, it appears difficult to secure stability with the hinge moment reduced to less than 25 percent of its value for the unbalanced surface.

2. Reduction of the floating moment C_{h_α}, if it can be brought about independently of a reduction of the aerodynamic balance, causes a shift of the boundary for divergence. (Cf. figs. 3 and 7 and figs. 12 and 13.) The effect is particularly noticeable in the case of the rudder, where the likelihood of this form of instability is materially decreased.

3. Within the usual range of characteristics, the elevator and the aileron controls are more susceptible to oscillatory instability than to the rapid form of divergent instability. The stability with either of these controls free may be improved by (*a*) using a less effective aerodynamic balance, (*b*) decreasing the mass moment and the moment of inertia of the control, or (*c*) using a control surface of narrow chord.

4. Divergence is a more likely form of instability for the rudder control (figs. 10 and 11) and may be avoided by reducing the effectiveness of the aerodynamic balance or, as has been suggested, by using a balance that reduces the floating tendency of the rudder, although a highly effective balance of a type that reduces the floating tendency may result in oscillatory instability.

5. The oscillatory stability of the elevator-free system is but little affected by the restoring moment of the airplane in pitch (C_{m_α}). In the case of the yawing motions, however, the existence of a strong restoring moment (C_{n_β}) increases the likelihood of oscillatory instability. (See, for example, fig. 10.)

6. In all cases, an increase in the relative radius of gyration of the airplane results in an increased range of stability (cf. figs. 3 and 4; see also fig. 10), but changes in weight without corresponding changes in the rotary inertia have little effect. (See fig. 5.)

7. The use of a narrow control surface is recommended as a means of increasing the control-free stability as well as from other considerations. The marked effect of reducing the chord is shown by a comparison of figure 8 with figure 3 and of figure 12 with figure 10.

LANGLEY MEMORIAL AERONAUTICAL LABORATORY,
NATIONAL ADVISORY COMMITTEE FOR AERONAUTICS,
LANGLEY FIELD, VA., *August 15, 1940.*

APPENDIX

STABILITY DERIVATIVES

The geometric and the aerodynamic characteristics used in the stability calculations are given in tables I to IV.

TABLE I.—GENERAL AIRPLANE CHARACTERISTICS

Tail length / Wing chord	2.75
Horizontal-tail area / Wing area	.158
Vertical-tail area / Wing area	.06
Horizontal-tail chord / Wing chord	.50
Vertical-tail chord / Wing chord	.333
Aileron chord / Wing chord	.15
Aileron span / Wing semispan	.50
Wing aspect ratio	6
Horizontal-tail aspect ratio	3.75
Vertical-tail aspect ratio	3.00

TABLE II.—ELEVATOR-FREE STABILITY COEFFICIENTS

	50-percent-chord elevator	25-percent-chord elevator
C_{L_α}	4.3	4.3
$C_{m_{D\phi}}$	−9.26	−9.26
$C_{m_{\alpha_{wing}}}$	$4.3(0.135-x_{a.c.})$	$4.3(0.135-x_{a.c.})$
$C_{m_{\alpha_{tail}}}$	−1.121	−1.121
$C_{m_{D\alpha}}$	−1.450	−1.450
C_{m_q}	−.960	−.672
$C_{m_{D\dot{\alpha}}}$	−.57	−.23
$C_{h_{D\delta}}$	−1.00	−.50
$C_{h_{D\phi}}$	−1.33	−.406
$C_{h_{\alpha_{tail}}}$	−0.24 and 0	−.075

TABLE III.—RUDDER-FREE STABILITY COEFFICIENTS

	50-percent-chord rudder	25-percent-chord rudder
C_{Y_β}	−0.274	−0.274
$C_{n_{D\phi}}$	−.582	−.582
C_{n_q}	−.0567	−.0397
$C_{n_{D\dot{\beta}}}$	−.0460	−.0175
$C_{h_{D\phi}}$	−.383	−.276
C_{h_β}	.123	.075
$C_{h_{D\delta}}$	−1.00	−.50

TABLE IV.—AILERON-FREE STABILITY COEFFICIENTS

	15-percent-chord aileron	30-percent-chord aileron
$C_{l_{D\phi}}$	−2.94	−2.94
C_{l_q}	−.229	−.352
$C_{l_{D\dot{\beta}}}$	−.110	−.295
$C_{h_{D\phi}}$	−.184	−.322
$C_{h_{D\delta}}$	−.650	−1.587

The aerodynamic coefficients are, in most cases, based on experimental results; theoretical values are used only where such results were not established. Discussions of the more commonly used derivatives will be found in references 7, 8, and 9. Several of the unfamiliar coefficients are developed in the following paragraphs.

Damping in pitching $C_{m_{D\theta}}$.—The principal component of damping in pitching, furnished by the horizontal tail, is

$$-\frac{l\dot{\theta}}{U_0}\frac{S_t l}{Sc}C_{L_{\alpha_t}}$$

In addition, the pitching motion introduces a relative camber of the wing section, giving rise to a moment coefficient

$$-\frac{\pi}{4}\frac{\dot{\theta}c}{2U_0}$$

Thus

$$C_m=-\frac{l\dot{\theta}}{U_0}\left(\frac{S_t l}{Sc}C_{L_{\alpha_t}}+\frac{\pi}{4}\frac{c}{2l}\right)$$

Then, since

$$\frac{l\dot{\theta}}{U_0}=\frac{2l}{c}D\theta$$

$$C_{m_{D\theta}}=-\left[2\frac{S_t}{S}\left(\frac{l}{c}\right)^2 C_{L_{\alpha_t}}+\frac{\pi}{4}\right]$$

Pitching-moment slope C_{m_α}.—The pitching-moment slope is given by

$$C_{m_\alpha}=-C_{L_\alpha}\frac{x_{a.c.}}{2}+C_L\frac{z_{a.c.}}{2}$$

where $x_{a.c.}$ and $z_{a.c.}$ are the distances of the aerodynamic center of the complete airplane behind and below the center of gravity. The location of the aerodynamic center for the airplane as a whole is estimated by taking the centroid of the aerodynamic centers of the various components. Thus, if terms in $z_{a.c.}$ (which is usually small) are neglected,

$$x_{a.c.}=x_{a.c._{wing}}+\frac{\alpha_t}{\alpha}\frac{C_{L_{\alpha_t}}}{C_{L_\alpha}}\frac{S_t}{S}\quad x_{a.c._{tail}}$$

Pitching-moment coefficient due to vertical acceleration $C_{m_{D\alpha}}$.—The pitching-moment coefficient due to vertical acceleration arises from the aerodynamic inertia of the wing and the horizontal tail surfaces in motion normal to their chords. The force on each surface is equal to the reaction of a body of air described by rotating the surface about its midchord line. Thus, the pitching moment

$$M=\left[\pi\rho\left(\frac{c}{2}\right)^2 b x_{50}+\pi\rho\left(\frac{c_t}{2}\right)^2 b_t x_{50_t}\right]\frac{dw}{dt}$$

and

$$C_m=\left[\frac{x_{50}}{c}+\frac{x_{50_t}}{c}\left(\frac{b_t c_t}{bc}\right)^2\right]\pi D\alpha$$

where x_{50} is the distance from the 50-percent-chord point of the wing to the center of gravity of the airplane and x_{50_t} is the same distance measured from the corresponding point of the horizontal tail.

Pitching moment due to elevator deflection C_{m_δ}.—The pitching moment due to elevator deflection is given by the formula

$$C_{m_\delta}=\frac{\partial C_m}{\partial\delta}=\frac{\partial\alpha_e}{\partial\delta}C_{L_{\alpha_t}}\frac{S_t}{S}\frac{l}{c}$$

where α_e is the angle of zero lift of the elevator.

Theoretical and experimental values for $\partial\alpha_e/\partial\delta$, for flaps with sealed hinges, are given in figure 15. The coefficients used in these calculations (C_{n_δ} and C_{l_δ} as well as C_{m_δ}) were, however, based on the experimentally determined changes of lift produced by a flap with open gaps at the hinges. The effect of a small gap is to reduce the effectiveness of the flap by about 30 percent. At a large deflection, the flap with inset-hinge balance shows a still greater loss because of the protruding balance portion.

Pitching-moment coefficient due to angular velocity of the elevator $C_{m_{D\delta}}$.—The pitching-moment coefficient due to angular velocity of the elevator is

$$C_{m_{D\delta}}=\frac{dC_{L_t}}{dD\delta}\frac{S_t}{S}\frac{l}{c}$$

where

$$\frac{dC_{L_t}}{dD\delta}=\frac{\partial C_{L_t}}{\partial D\delta}+\frac{\partial\alpha_e}{\partial D\delta}\frac{dC_{L_t}}{d\alpha_t}$$

The parameters $\partial C_{L_t}/\partial D\delta$ and $\partial\alpha_e/\partial D\delta$ may be found as functions of the chordwise position of the hinge from figure 15. The figure is based on the theoretical treatment of Theodorsen (reference 7), with the assumption of long oscillations (greater than 20 chord lengths). It must be remembered that $D\delta$ involves the distance traveled by the airplane measured in terms of its half-wing chord, and the quantities given must be multiplied by the ratio c_t/c_w to convert them to half-wing chord lengths.

Damping moment of elevator $C_{h_{D\delta}}$.—The hinge moment due to angular velocity is treated theoretically by Theodorsen in reference 7. Figure 16, derived from the theory, gives the component parameters of the damping moment as functions of the chordwise position of the hinge. The same considerations are effective here as in the application of figure 15.

Hinge moment due to pitching $C_{h_{D\delta}}$.—Positive pitching motion causes an increase in the angle of attack of the tail surface equal to $l\dot{\theta}/U_0$. The resulting hinge-moment coefficient is

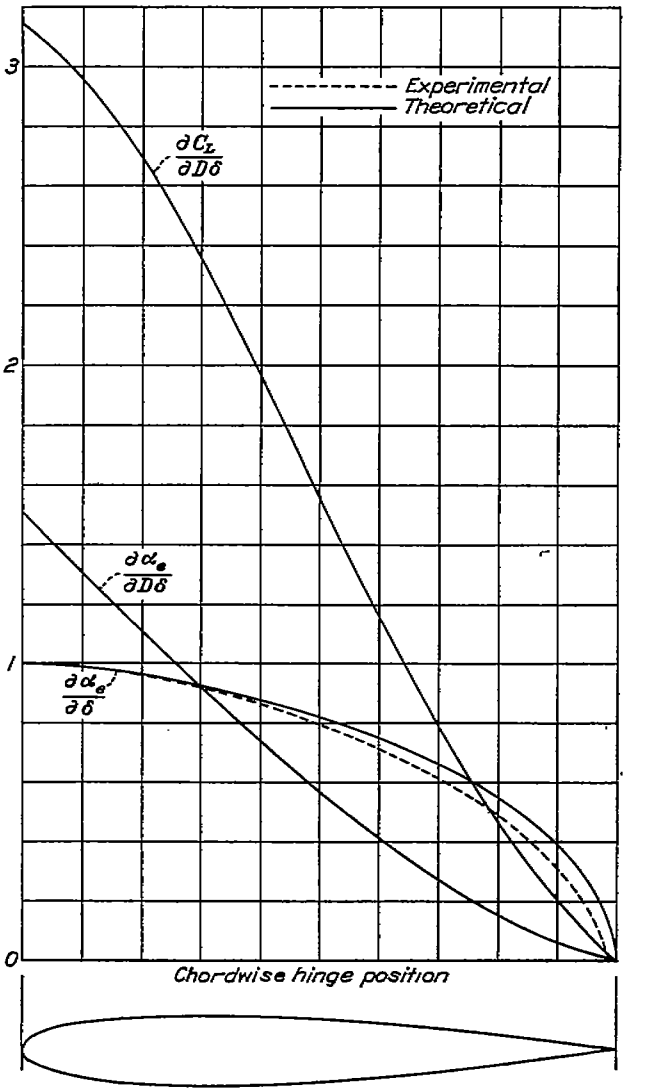

FIGURE 15.—Parameters for determining the effects of angular velocity and deflection of flaps on the lift.

$$C_L=D\delta\frac{\partial C_L}{\partial D\delta}+D\delta\frac{\partial C_L}{\partial\alpha}\frac{\partial\alpha_e}{\partial D\delta}+\delta\frac{\partial C_L}{\partial\alpha}\frac{\partial\alpha_e}{\partial\delta}$$

$$\frac{l\dot{\theta}}{U_0}C_{h_{\alpha_{tail}}}$$

and, since

$$\frac{l\dot{\theta}}{U_0}=\frac{2l}{c}D\theta$$

$$C_{h_{D\delta}}=\frac{2l}{c}C_{h_{\alpha_{tail}}}$$

Inasmuch as rotation of the airplane about its center of gravity does not appreciably change the lift of the wing, the downwash correction may be neglected.

Hinge moment due to change in angle of attack C_{h_α}.—In accordance with the indications of tests by Goett and Reeder (reference 4), the aerodynamic floating moment $C_{h_{\alpha_{tail}}}$ was assumed independent of the degree of aerodynamic balance of the control surface

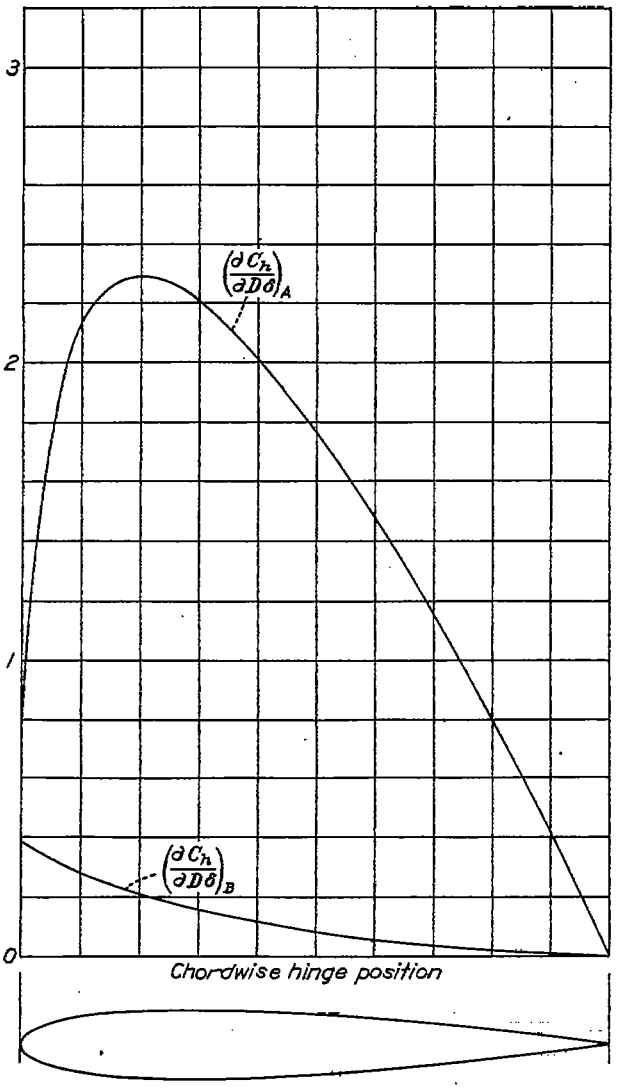

FIGURE 16.—Parameters for determining the damping moments of flaps.

$$C_{h_{D\delta}}=\left(\frac{\partial C_h}{\delta D\delta}\right)_A+\frac{dC_L}{d\alpha}\left(\frac{\partial C_h}{\delta D\delta}\right)_B$$

(fig. 6). The assumption is valid for the inset-hinge type of balanced flap shown in this figure. The floating moment will vary with the type of balance, however, as discussed in the text, and additional computations were therefore made in which $C_{h_{\alpha_{tail}}}$ was assumed equal to zero.

The lateral-stability derivatives C_{Y_β}, C_{n_β}, $C_{n_{D\psi}}=\frac{\partial C_n}{\partial\frac{rc}{2U_0}}$, and $C_{l_{D\phi}}=\frac{\partial C_l}{\partial\frac{pc}{2U_0}}$ are discussed in references 8 and 9. The other coefficients for the lateral motions are derived in a manner closely analogous to the derivation of the corresponding longitudinal coefficients.

The values of the mass moment and the moment-of-inertia coefficients of several representative elevator-control systems were determined experimentally in order to find the magnitude and the range to be expected in practice. The experiments were made by attaching a spring of known stiffness to the control column, oscillating the system, and recording the frequency and the damping. The mass moment was measured directly with a spring scale. The interpreted results are given in the following table:

Airplane	$\mu_e\overline{x}$	$\mu_e k_e^2$
North American BT-9	2.70	1.35
Curtiss P-36	0	.90
Lockheed 12	9.5	4.5
Fairchild 22	8.0	1.1

REFERENCES

1. Bartsch, Edmund: Wende- und Rollschwingungen eines Flugzeugs. Jahrb. 1938 der deutschen Versuchsanstalt für Luftfahrt, E. V. (Berlin-Adlershof) pp. 179–194.
2. Jeffreys, Harold: Operational Methods in Mathematical Physics. Cambridge Tracts in Mathematics and Mathematical Physics, No. 23, 2d ed., Cambridge Univ. Press, 1931.
3. Jones, Robert T., and Fehlner, Leo F.: Transient Effects of the Wing Wake on the Horizontal Tail. T. N. No. 771, NACA, 1940.
4. Goett, Harry J., and Reeder, J. P.: Effects of Elevator Nose Shape, Gap, Balance, and Tabs on the Aerodynamic Characteristics of a Horizontal Tail Surface. Rep. No. 675, NACA, 1939.
5. Hemphill, T. M.: Control Surface Hinge Moments and Their Relation to Stability. Paper presented before Inst. Aero. Sci., New York, Jan. 26, 1940.
6. Pugsley, A. G.: Aileron Stability, with Special Reference to Rolling-Aileron Motion and the Influence of Frise Type Hinge Moment Curves. R. & M. No. 1595, British A. R. C., 1934.
7. Theodorsen, Theodore: General Theory of Aerodynamic Instability and the Mechanism of Flutter. Rep. No. 496, NACA, 1935.
8. Zimmerman, Charles H.: An Analysis of Lateral Stability in Power-Off Flight with Charts for Use in Design. Rep. No. 589, NACA, 1937.
9. Weick, Fred E., and Jones, Robert T.: The Effect of Lateral Controls in Producing Motion of an Airplane as Computed from Wind-Tunnel Data. Rep. No. 570, NACA, 1936.